

# The influence of $\text{SrSO}_4$ on the tribological properties of $\text{NiCr-Al}_2\text{O}_3$ cermet at elevated temperatures

Feng Liu<sup>a,b</sup>, Gewen Yi<sup>a</sup>, Wenzhen Wang<sup>a</sup>, Yu Shan<sup>a</sup>, Junhong Jia<sup>a,\*</sup>

<sup>a</sup>State Key Laboratory of Solid Lubrication, Lanzhou Institute of Chemical Physics, Chinese Academy of Sciences, Lanzhou 730000, PR China

<sup>b</sup>University of Chinese Academy of Sciences, Beijing 100039, PR China

Received 6 September 2013; received in revised form 1 October 2013; accepted 7 October 2013

Available online 18 October 2013

## Abstract

The tribological properties of  $\text{NiCr-40 wt\%Al}_2\text{O}_3$  (NC40A) cermet-based self-lubricating composites containing 10 wt%–30 wt%  $\text{SrSO}_4$  against alumina ball were investigated at elevated temperatures. The results indicated that the friction coefficients and wear rates were significantly reduced by adding different amounts of  $\text{SrSO}_4$  above 200 °C. NC40A–10 $\text{SrSO}_4$  composite exhibited satisfactory tribological properties above 200 °C due to the formation of synergistic lubricating films  $\text{SrAl}_4\text{O}_7$  and  $\text{NiCr}_2\text{O}_4$  on the contact surface, while low friction coefficient and wear rate of NC40A–30 $\text{SrSO}_4$  composite at 400 °C were attributed to the synergistic lubricating effect of  $\text{Sr}_4\text{Al}_2\text{O}_7$ ,  $\text{SrAl}_2\text{O}_4$  and  $\text{NiCr}_2\text{O}_4$ .

© 2013 Elsevier Ltd and Techna Group S.r.l. All rights reserved.

**Keywords:** Self-lubricating composites; Synergistic lubrication; Elevated temperature; Tribological properties

## 1. Introduction

High temperature self-lubricating composites are promising potential for the tribology community in turbine construction and aerospace systems owing to extraordinary lubricating properties at elevated temperatures [1,2]. A lot of research works have been done on nickel alloys and ceramics containing solid lubricants during the past few years [3–10]. However, traditional solid lubricants such as graphite and molybdenum disulfide will lose lubricating function at high temperature due to their chemical and/or structural degradations, while alkali earth fluorides ( $\text{CaF}_2$  and  $\text{BaF}_2$ ) exhibit low friction coefficient at elevated temperature. Oxides are generally hard to shear at room temperature, but some of them become highly shearable and hence can provide fairly low friction coefficients at elevated temperatures [11]. In order to achieve lubrication over a broader temperature range, a number of researchers have made efforts to improve self-lubricating composites. The way to produce a lubricating layer that can operate over a wide temperature range is to combine low- and high-

temperature lubricants into the composites [12]. For example, at higher temperature, the formation of  $\text{PbMoO}_4$  or  $\text{ZnWO}_4$  on the sliding surface, which facilitated by combining certain transition metal dichalcogenides ( $\text{MoS}_2$  or  $\text{WS}_2$ ) with oxides ( $\text{PbO}$  or  $\text{ZnO}$ ), was apparently beneficial to providing good lubrication at this temperature [13,14]. Molybdates and vanadates were well known for their lubricating properties [15,16]. For example, the formation of silver molybdates and silver vanadates on the contact surface were found to exhibit relatively low friction coefficient at elevated temperature in  $\text{Mo}_2\text{N}/\text{MoS}_2/\text{Ag}$  [17,18] and  $\text{VN}/\text{Ag}$  [19] systems, which was due to the chemical reaction that combined silver and molybdenum oxide or vanadium oxide.  $\text{CaSO}_4$  film exhibited a low coefficient of friction at 500 °C, which was attributed to the tribo-chemical reaction between  $\text{CaF}_2$  and  $\text{WS}_2$  on the rubbing surface [20]. Molybdenum disulfide would decompose in the process of hot pressing when it was used as additive in the metal-based composite, which induced its lubricating function lost partly, but the formation of  $\text{Cr}_x\text{S}_{x+1}$  would provide excellent lubricating properties [4].

For high self-lubricating composites, as powder metallurgical materials containing solid lubricants, the continuity of the composites was destroyed by soft solid lubricants and some

\*Corresponding author. Tel.: +86 931 4968611; fax: +86 931 8277088.

E-mail address: [jhjia@licp.cas.cn](mailto:jhjia@licp.cas.cn) (J. Jia).

solid lubricants might be melt, oxidize or decompose at high sintering temperature, which damaged their lubricating properties drastically [21,22]. Based on the method for the formation of the lubricating layer on the rubbing surface, moderate interfacial reaction between the matrix and lubricants not only avoided poor interfacial bonds, but also resulted in improved tribological properties, which might be attributed to the formation of reaction products in the sintering process. In our previous study, due to the reaction between NC40A matrix and  $\text{SrSO}_4$  in the process of hot pressing, NC40A10S composite exhibited satisfactory tribological properties above 200 °C, which was attributed to the formation of synergistic lubricating films  $\text{SrAl}_4\text{O}_7$  and  $\text{NiCr}_2\text{O}_4$  on the rubbing surface [23]. According to the phase diagram, five intermediate compounds, i.e.,  $\beta\text{-4SrO} \bullet \text{Al}_2\text{O}_3$ ,  $3\text{SrO} \bullet \text{Al}_2\text{O}_3$ ,  $\text{SrO} \bullet \text{Al}_2\text{O}_3$ ,  $\text{SrO} \bullet 2\text{Al}_2\text{O}_3$ ,  $\text{SrO} \bullet 6\text{Al}_2\text{O}_3$  exist in the  $\text{SrO}\text{--}\text{Al}_2\text{O}_3$  system [24]. Therefore, it is necessary to evaluate the effects of  $\text{SrSO}_4$  contents on the tribological properties of the sintered composites at elevated temperatures. In this paper, NiCr–40 wt%  $\text{Al}_2\text{O}_3$  cermet-based self-lubricating composites with different amounts of  $\text{SrSO}_4$  were prepared by powder metallurgy (P/M) and their tribological properties were investigated by a ball-on-disk tribometer against alumina ball from room temperature to 800 °C. Meanwhile, the effects of  $\text{SrSO}_4$  contents on the tribological properties and wear mechanisms of the sintered composites were analyzed and discussed.

## 2. Experiment details

The NiCr–40 wt%  $\text{Al}_2\text{O}_3$  cermet (denoted by NC40A) was fabricated by vacuum-hot-pressing furnace (ZT–45–20Y, Shanghai Chen Hua Electric Furnace Corp Ltd., China).  $\text{SrSO}_4$  was incorporated into the NC40A cermet. The composition of NiCr– $\text{Al}_2\text{O}_3$  cermet-based composites was shown in Table 1. The starting materials were a commercially available Ni (60  $\mu\text{m}$ , 99.5% purity), Cr (45  $\mu\text{m}$ , 99.95% purity),  $\alpha\text{-Al}_2\text{O}_3$  (30 nm, 99.99% purity),  $\text{SrSO}_4$  (99.7% purity), all in form of powders. Ni (80 wt%) and Cr (20 wt%) powders were first ball-milled for 20 h in Pulverisette 5 Planetary high-energy-mill (Fritsch, Germany), then  $\text{Al}_2\text{O}_3$  and  $\text{SrSO}_4$  were added and continuously ball-milled for 20 h. The ratio of ball to powders was 10:1 in weight. The milled powders were then cold compacted in a graphite die at a pressure of 20 MPa. Then, the pressed specimens were sintered at 1100–1150 °C for 1 h with a heating rate of 10 °C/min under the pressure of

25 MPa in a hot press sintering furnace at a dynamic vacuum of about  $10^{-2}$  Pa. The specimens were machined and polished into designed samples for following analyses and tests.

The density of the sintered composites was determined by using a helium pycnometry (AccuPyc 1330, Micromeritics Int. Corp., USA) after calculating the volume. The hardness measurements were conducted using MH–5 Vickers microhardness instrument with a load of 300 g and a dwell time of 10 s, and the average value of ten repeat tests was given in this article. The friction and wear tests of the sintered composites were carried out on a high temperature tribometer with a ball-on-disk configuration (CSM Instruments LTD, Switzerland). The disk was the sintered composites with the size of  $\Phi 40 \text{ mm} \times 8 \text{ mm}$  and the friction surface was polished to a roughness of 0.05  $\mu\text{m}$ , while the counterpart ball with a diameter of 3 mm was made of  $\text{Al}_2\text{O}_3$  ceramic (Shanghai Unite Technology Co. Ltd., China). The chemical composition (wt%) of  $\text{Al}_2\text{O}_3$  ball was 99.5%  $\text{Al}_2\text{O}_3$  and 0.5% sintering aids ( $\text{SiO}_2$ ,  $\text{MgO}$ ,  $\text{Fe}_2\text{O}_3$  and  $\text{Na}_2\text{O}$ ). The  $\text{Al}_2\text{O}_3$  ball has a surface roughness of 0.032  $\mu\text{m}$ , a hardness of 16.5 GPa, and density of 3.92  $\text{g/cm}^3$ . All the friction and wear tests were run at a sliding velocity of 0.1 m/s, normal load of 10 N, duration of 60 min, wear track radius of 5 mm and the selected test temperatures were RT, 200 °C, 400 °C, 600 °C, 800 °C. The wear depth profiles of all the wear tracks were examined by Nano Map 500LS contact surface mapping profiler (AEP Technology, USA) to obtain wear rate of composites. All the tribological tests were carried out at least three times to make sure the reproducibility of the experimental results under the same condition, and the average results were reported. The phase compositions of the composites and worn surfaces were analyzed by Rigaku D/max-RB X-ray diffractometer (XRD) with 40 kV operating voltage and Cu  $K\alpha$  radiation in the  $2\theta$  range of 19–80°. The microstructures and morphologies of worn surfaces were characterized by JSM–5600LV scanning electron microscope equipped with energy dispersive spectroscopy (EDS).

## 3. Results

### 3.1. XRD analyses of the composites

Fig. 1 shows the XRD patterns of NC40A cermet-based composites with different amounts of  $\text{SrSO}_4$  before and after sintering. It can be seen that the noticeable changes of phase composition in final composites with different amounts of  $\text{SrSO}_4$ , which is ascribed to the chemical reaction between  $\text{Al}_2\text{O}_3$  and  $\text{SrO}$  deriving from the decomposition of  $\text{SrSO}_4$  during sintering process. For NC40A–10 $\text{SrSO}_4$  composite, it is confirmed that the phase organization of the sintered composite contains Ni (Cr) solid solution,  $\alpha\text{-Al}_2\text{O}_3$ ,  $\text{SrAl}_4\text{O}_7$ ,  $\text{NiCr}_2\text{O}_4$  and  $\text{Cr}_2\text{O}_3$  [23]. With the further addition of  $\text{SrSO}_4$ , the corresponding to the XRD patterns of NC40A–20 $\text{SrSO}_4$  composite reveals that  $\text{Sr}_4\text{Al}_2\text{O}_7$  and  $\text{SrAl}_2\text{O}_4$  are formed in the sintered composite. However, the diffraction peaks of  $\text{SrAl}_2\text{O}_4$  are weak. It has been reported that  $\text{Sr}_3\text{Al}_2\text{O}_6$  was formed from the reaction between  $\text{SrO}$  and  $\text{Al}_2\text{O}_3$  in the

Table 1  
Chemical compositions, sintering parameters, density and microhardness of NiCr40A cermet-based composites with various amount of  $\text{SrSO}_4$ .

Composition (wt%)	PM sintering parameters (°C, h, MPa)	Density ( $\text{g/cm}^3$ )	Vickers hardness (HV)
NC40A	1300, 1, 25	5.68	1082 $\pm$ 47
NC40A–10 $\text{SrSO}_4$	1100, 1, 25	5.29	235 $\pm$ 22
NC40A–20 $\text{SrSO}_4$	1150, 1, 25	4.25	224 $\pm$ 19
NC40A–30 $\text{SrSO}_4$	1150, 1, 25	4.09	269 $\pm$ 11

temperature range from 1000 °C to 1200 °C [25], while  $\text{Sr}_3\text{Al}_2\text{O}_6$  was transformed into  $\text{Sr}_4\text{Al}_2\text{O}_7$  at 1130 °C and the  $\beta$ -phase of  $\text{Sr}_4\text{Al}_2\text{O}_7$  was stable from 1130 °C to 1450 °C [26]. In addition,  $\text{SrAl}_2\text{O}_4$  was obtained over a wide temperature range from 900 °C to 1400 °C [27]. Therefore, it is reasonable to assume that the following simplified chemical reaction occurs,



when the content of  $\text{SrSO}_4$  up to 30 wt%, the diffraction peaks of  $\text{SrAl}_2\text{O}_4$  become intense in the sintered composites. It is expected that the new phases of  $\text{Sr}_4\text{Al}_2\text{O}_7$ ,  $\text{SrAl}_2\text{O}_4$  and  $\text{NiCr}_2\text{O}_4$  will play an important role in the formation of lubricating films on the sliding surface, which might be lead to a decrease in the friction coefficients and wear rates of the composites at a wide temperature range.

### 3.2. Hardness, density and microstructure analyses of composites

The microhardness and density of NC40A cermet-based composites are shown in Table 1. It is observed that the microhardness of NC40A cermet holds a high hardness of  $1082 \pm 47$  HV. The microhardness of NC40A cermet is dramatically reduced by the incorporation of  $\text{SrSO}_4$  lubricant, where the microhardness of NC40A–10 $\text{SrSO}_4$  composite is about  $235 \pm 22$  HV. With the further addition of  $\text{SrSO}_4$ , the microhardness of the composites exhibits slightly decrease, then increases to  $269 \pm 11$  HV at 30 wt %  $\text{SrSO}_4$  concentrations. As shown in Table 1, it can be seen that the density of the sintered composites decreases with the increase of  $\text{SrSO}_4$  content. Microstructures of NC40A cermet-based composites with different amounts of  $\text{SrSO}_4$  are shown in Fig. 2. As shown in Fig. 2a, it can be seen that the dispersed gray phases are homogeneously distributed throughout NC40A–10 $\text{SrSO}_4$  composite. EDS analysis and XRD results demonstrate that the gray phases are Ni (Cr) solid solution and the dark gray phases are  $\text{Al}_2\text{O}_3$ ,  $\text{Cr}_2\text{O}_3$ ,  $\text{SrAl}_4\text{O}_7$  and  $\text{NiCr}_2\text{O}_4$ . The NC40A–20 $\text{SrSO}_4$  and NC40A–30 $\text{SrSO}_4$  composites exhibit similar morphologies, consisting of Ni (Cr) solid solution (the gray phase),  $\text{Al}_2\text{O}_3$ ,  $\text{Cr}_2\text{O}_3$ ,

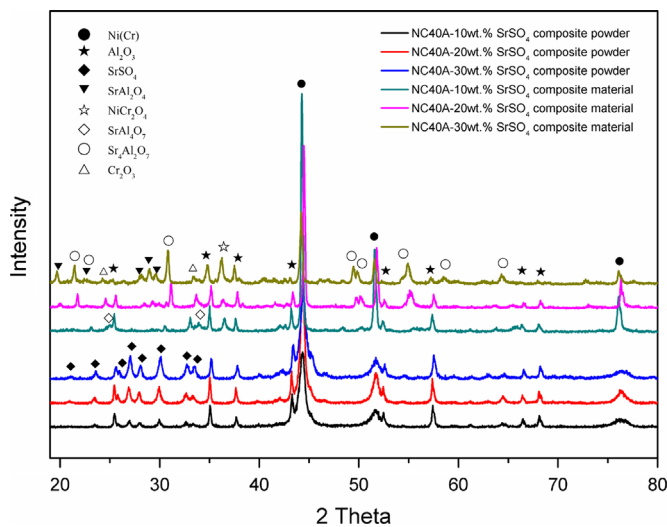


Fig. 1. XRD patterns of NC40A cermet-based composites before and after hot-pressing.

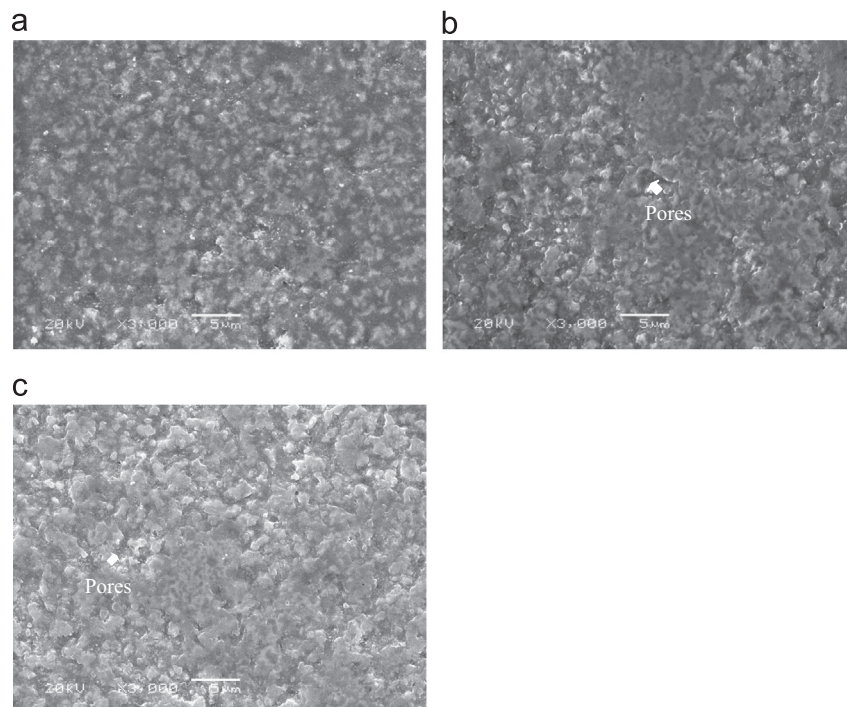


Fig. 2. SEM micrographs of (a) NC40A–10 $\text{SrSO}_4$  composite, (b) NC40A–20 $\text{SrSO}_4$  composite, and (c) NC40A–30 $\text{SrSO}_4$  composite.



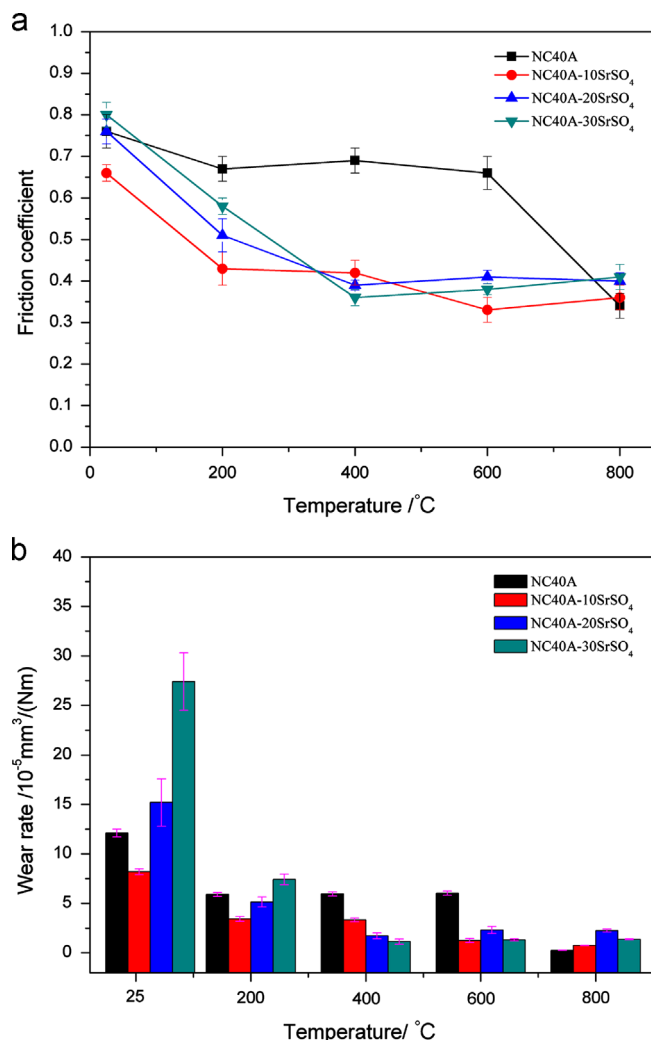


Fig. 3. Tribological properties of NC40A cermet with and without SrSO<sub>4</sub> at load 10 N, sliding velocity 0.1 m/s against alumina ball as a function of the test temperature: (a) friction coefficient, and (b) wear rate.

Sr<sub>4</sub>Al<sub>2</sub>O<sub>7</sub>, SrAl<sub>2</sub>O<sub>4</sub> and NiCr<sub>2</sub>O<sub>4</sub> (the dark gray phase). However, it can be seen that the formation of Sr<sub>4</sub>Al<sub>2</sub>O<sub>7</sub> and SrAl<sub>2</sub>O<sub>4</sub> in the process of hot pressing leads to many pores in the sintered composites. It is confirmed that strontium aluminates (Sr<sub>4</sub>Al<sub>2</sub>O<sub>7</sub> and SrAl<sub>2</sub>O<sub>4</sub>) might be harmful for the integrity of the composites.

### 3.3. Tribological property of the composites against alumina ball

The variations of friction coefficient and wear rate of NC40A cermet-based composites with different amounts of SrSO<sub>4</sub> as a function of the test temperature are shown in Fig. 3. As shown in Fig. 3, NC40A cermet exhibits relatively high friction coefficient combined with high wear rate in the temperature range from room temperature to 600 °C. However, the friction coefficient and wear rate decrease to 0.34 and  $2.62 \times 10^{-6}$  mm<sup>3</sup>/Nm at 800 °C. When the addition of 10 wt% SrSO<sub>4</sub> in NC40A cermet, the friction coefficient and wear rate decrease obviously with the increase in the test temperature and are lower than the pristine composite. However, its tribological properties

at room temperature are still very poor. In order to further improve tribological properties of NC40A cermet, the composite with 20 wt% SrSO<sub>4</sub> is investigated. It is observed that the friction coefficient of the sintered composite is as high as 0.76 at room temperature, but gradually decreases to 0.39 at 400 °C, then increases around 0.4 between 600 °C and 800 °C. Compared to NC40A cermet, the sintered composite exhibits high wear rate at room temperature, then its wear rate reaches to a minimum value of  $1.72 \times 10^{-6}$  mm<sup>3</sup>/Nm at 400 °C. With further increase in the test temperature, the wear rate of the composite remains the level of  $2.31 \times 10^{-5}$  mm<sup>3</sup>/Nm. The further addition of SrSO<sub>4</sub> can lower the friction coefficient and wear rate of NC40A cermet at 400 °C, but the friction coefficient and wear rate of NC40A–30SrSO<sub>4</sub> composite are getting worse at room temperature, which was attribute to formation of Sr<sub>4</sub>Al<sub>2</sub>O<sub>7</sub>, SrAl<sub>2</sub>O<sub>4</sub> and NiCr<sub>2</sub>O<sub>4</sub> during sintering process. Above 400 °C, the friction coefficient of NC40A–30SrSO<sub>4</sub> composite also remains around 0.4 as same as NC40A–20SrSO<sub>4</sub> composite, while its wear rate was lower than that of NC40A–20SrSO<sub>4</sub> composite. It is evident that NC40A–10SrSO<sub>4</sub> composite exhibits good tribological properties over a wide temperature range from 200 °C to 800 °C.

### 3.4. Worn surfaces analysis of the composites

The worn surface morphologies of NC40A–10SrSO<sub>4</sub> composite after wear tests at different temperatures are shown in Fig. 4. At the room temperature, the worn surface appears to be covered with a thin smeared tribofilm, some cracks and light grooves are also observed in the wear track, suggesting that the wear mechanism is characterized by micro-plowing (Fig. 4a). At 200 °C and 400 °C, the worn surface is characterized by the discontinuous lubricating films, these discontinuous films are deformed, and containing large delamination pits (Fig. 4b and c). The wear mechanism of the composite is characterized by plastic deformation and micro-plowing. With the increase in the test temperature, the worn surface is covered by continuous lubricating films, and plowed grooves and small delamination pits appear in the wear tracks (Fig. 4d and e). It indicates that the wear mechanism is mainly in the form of micro-plowing and the reduced friction and wear is attributed to the formation of lubricating films at elevated temperatures.

Fig. 5 shows the worn surfaces morphologies of NC40A–20SrSO<sub>4</sub> composite after wear tests at different temperatures. At room temperature, significant brittle fracture of the worn surface occurs and light grooves are formed parallel to the sliding direction. Also, crack initiation, crack propagation and connection appear on the worn surface of the sintered composite, which was attributed to formation of Sr<sub>4</sub>Al<sub>2</sub>O<sub>7</sub>, SrAl<sub>2</sub>O<sub>4</sub> and NiCr<sub>2</sub>O<sub>4</sub> during sintering process. As shown in Fig. 5b and c, at 200 °C and 400 °C, the worn surface is relatively smooth with plastic deformation and delamination pits, and there is no evidence that the surface cracks are observed. The plastic deformation and micro-plowing are considered to the dominated wear mechanism. Above 600 °C, the worn surface is covered with continuous glaze film as well as with distinct spoors of plastic deformation, and

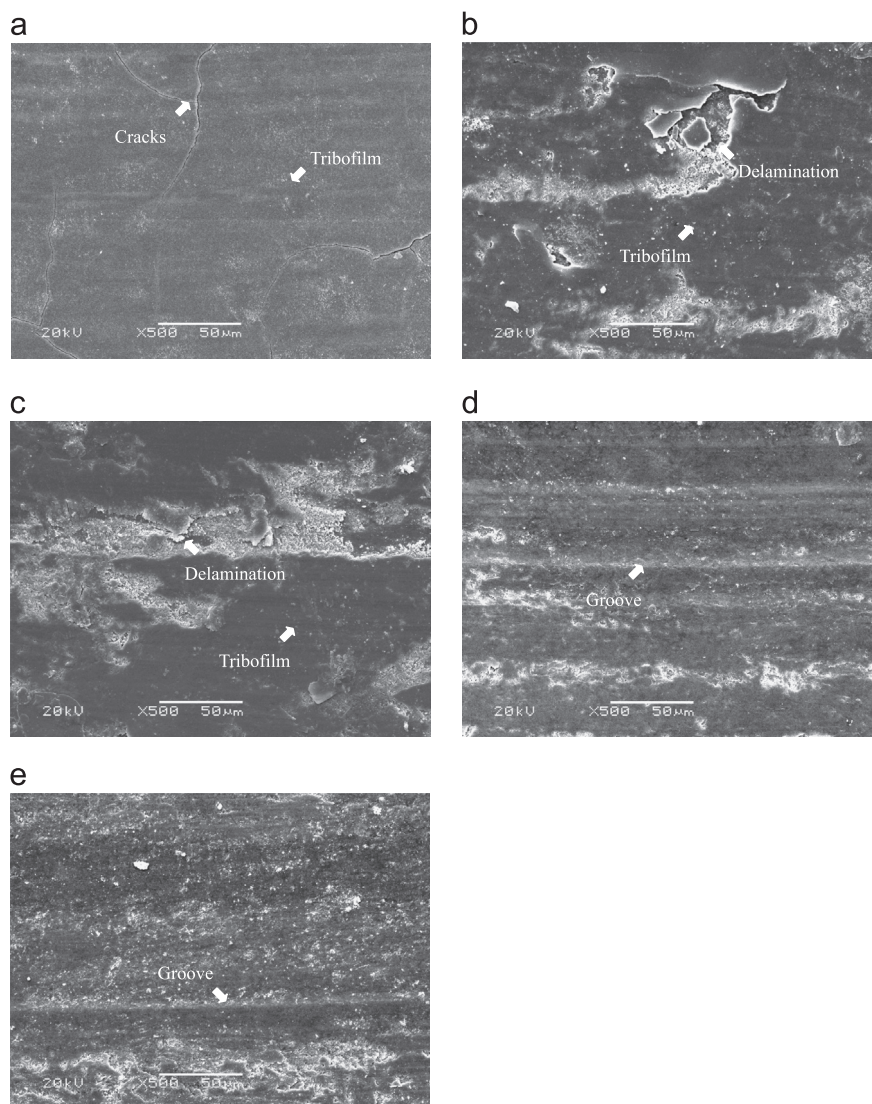


Fig. 4. SEM morphologies of worn surfaces of NC40A–10SrSO<sub>4</sub> composite after wear tests at different temperatures: (a) room temperature, (b) 200 °C, (c) 400 °C, (d) 600 °C, and (e) 800 °C.

the glaze film turns smooth with the increase in the test temperature. It is evident that the formation of Sr<sub>4</sub>Al<sub>2</sub>O<sub>7</sub>, SrAl<sub>2</sub>O<sub>4</sub> and NiCr<sub>2</sub>O<sub>4</sub> in the process of hot pressing provides good tribological properties above 200 °C.

Fig. 6 shows the worn surfaces morphologies of NC40A–30SrSO<sub>4</sub> composite after wear tests at different temperatures. At room temperature, the worn surface is characterized by light parallel grooves with typical brittle fracture and delamination pits. It is responsible for an increase in wear rate at room temperature. As temperature increases to 200 °C, the worn surface is covered with discontinuous tribofilm and some delamination pits. The wear mechanism is characterized by micro-plowing and plastic deformation. When the temperature up to above 400 °C, the worn surface is covered with continuous glaze layer and light grooves parallel to the sliding direction on the worn surfaces of the sintered composites, and the continuous glaze layer turns smooth with the increase in the test temperature due to the effective spreading of synergistic lubricating film on the contact surface, which leads to a

distinct decrease in the friction coefficient and wear rate at 400 °C and 600 °C as compared to NC40A cermet (Fig. 3).

Fig. 7 shows XRD patterns of the worn surfaces of NC40A cermet-based composites with different amount of SrSO<sub>4</sub> after wear tests at different temperatures. For NC40A–10SrSO<sub>4</sub> composite, it can be found that Ni(Cr) solution, Al<sub>2</sub>O<sub>3</sub>, Cr<sub>2</sub>O<sub>3</sub>, SrAl<sub>4</sub>O<sub>7</sub>, and NiCr<sub>2</sub>O<sub>4</sub> phases are identified on the worn surfaces of the sintered composites below 800 °C, and the diffraction peaks of NiO are detected on the worn surfaces of the composites above 600 °C (Fig. 7a). As shown in Fig. 7b, it can be seen that the existence of Ni(Cr) solution, Al<sub>2</sub>O<sub>3</sub>, Cr<sub>2</sub>O<sub>3</sub>, Sr<sub>4</sub>Al<sub>2</sub>O<sub>7</sub>, SrAl<sub>2</sub>O<sub>4</sub> and NiCr<sub>2</sub>O<sub>4</sub> phases on the worn surface of NC40A–20SrSO<sub>4</sub> composite at different test temperatures except the oxidation of Ni and Cr above 600 °C. The diffraction peaks as same as those of NC40A–20SrSO<sub>4</sub> composite are observed on the worn surface of NC40A–30SrSO<sub>4</sub> composite at different test temperatures (Fig. 7c). It is confirmed that the phases in the sintered composites do not react with each other during the high temperature test process.

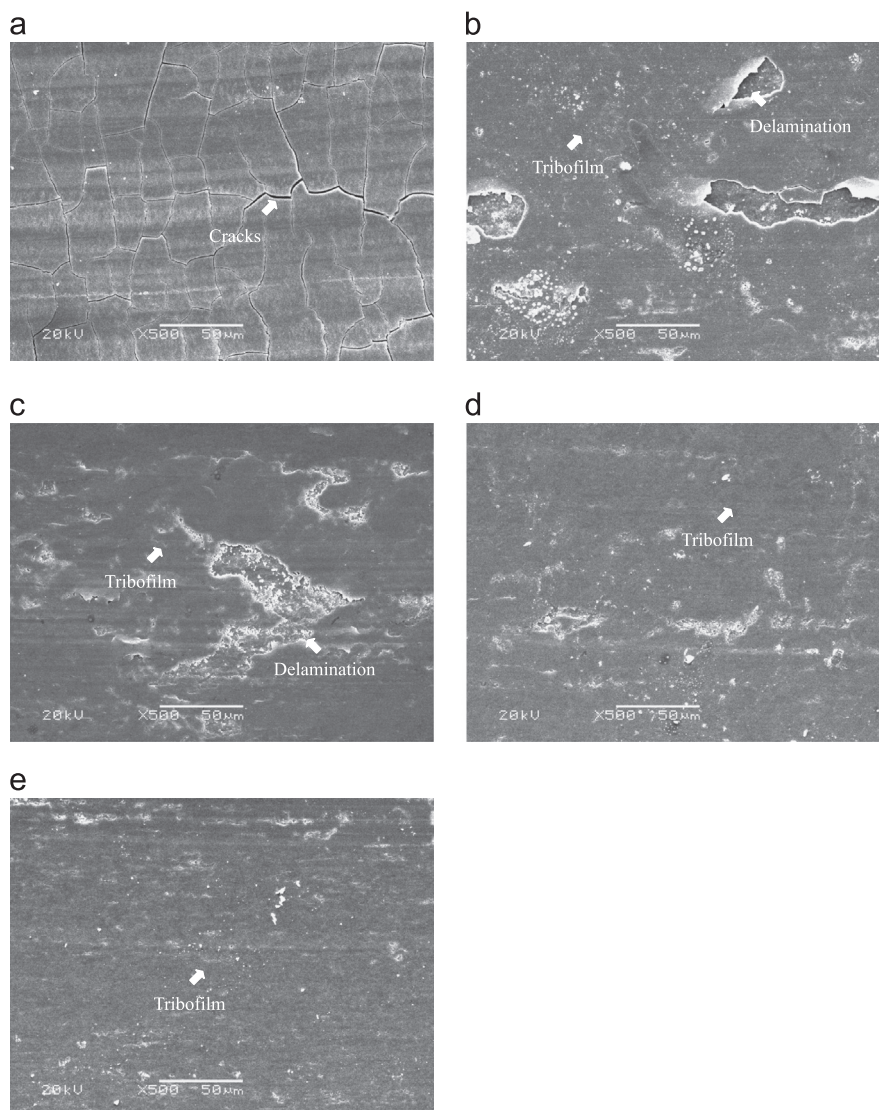


Fig. 5. SEM morphologies of worn surfaces of NC40A–20SrSO<sub>4</sub> composite after wear tests at different temperatures: (a) room temperature, (b) 200 °C, (c) 400 °C, (d) 600 °C, and (e) 800 °C.

#### 4. Discussion

As seen in Fig. 3, it indicated that NC40A–SrSO<sub>4</sub> composites exhibited good tribological performance over a wide temperature range from 200 °C to 600 °C as compared to the NC40A cermet, which was ascribed to the formation of SrAl<sub>4</sub>O<sub>7</sub>, Sr<sub>4</sub>Al<sub>2</sub>O<sub>7</sub>, SrAl<sub>2</sub>O<sub>4</sub> and NiCr<sub>2</sub>O<sub>4</sub> during sintering process. However, the tribological properties of NC40A–SrSO<sub>4</sub> composites were very poor at room temperature. As shown in Figs. 4–6a, it can be seen that some cracks appeared on the worn surface of the sintered composites. This further supported observation that the formation of Sr<sub>4</sub>Al<sub>2</sub>O<sub>7</sub>, SrAl<sub>2</sub>O<sub>4</sub> and NiCr<sub>2</sub>O<sub>4</sub> in the sintered products made the composites brittle. Therefore, when the contents of SrSO<sub>4</sub> are more than 20 wt%, the sintered composites exhibited typical brittle fracture on the worn surface, resulting in a higher wear rate than that of NC40A cermet at room temperature. At 200 °C, the composites exhibited lower friction coefficient and no distinct cracks, discontinuous glaze layer and delamination were observed

on the worn surface, which might be attributed to the formation of the lubricating films on the contact surface. Mild plastic deformation of the sintered composites and the formation of discontinuous synergistic lubricating film were the dominated wear mechanism at 200 °C. When the temperature up to 400 °C, the lubricating films on worn surface became very smooth with the increase in the content of SrSO<sub>4</sub>, especially NC40A–30SrSO<sub>4</sub> composite (Fig. 6c). Therefore, NC40A–30SrSO<sub>4</sub> composite exhibited extraordinary tribological properties due to the formation of the lubricating films Sr<sub>4</sub>Al<sub>2</sub>O<sub>7</sub>, SrAl<sub>2</sub>O<sub>4</sub> and NiCr<sub>2</sub>O<sub>4</sub> on the worn surface at 400 °C (Fig. 3). Between 600 °C and 800 °C, according to XRD analysis of the worn surfaces, the oxides were observed on the rubbing surface, and NC40A–10SrSO<sub>4</sub> composite exhibited satisfactory tribological properties. However, the friction coefficient and wear rate were not reduced by further addition of SrSO<sub>4</sub> under this experimental condition because of severe adhesive transfer of NC40A–20SrSO<sub>4</sub> and NC40A–30SrSO<sub>4</sub> composites. Between 600 °C and 800 °C, the



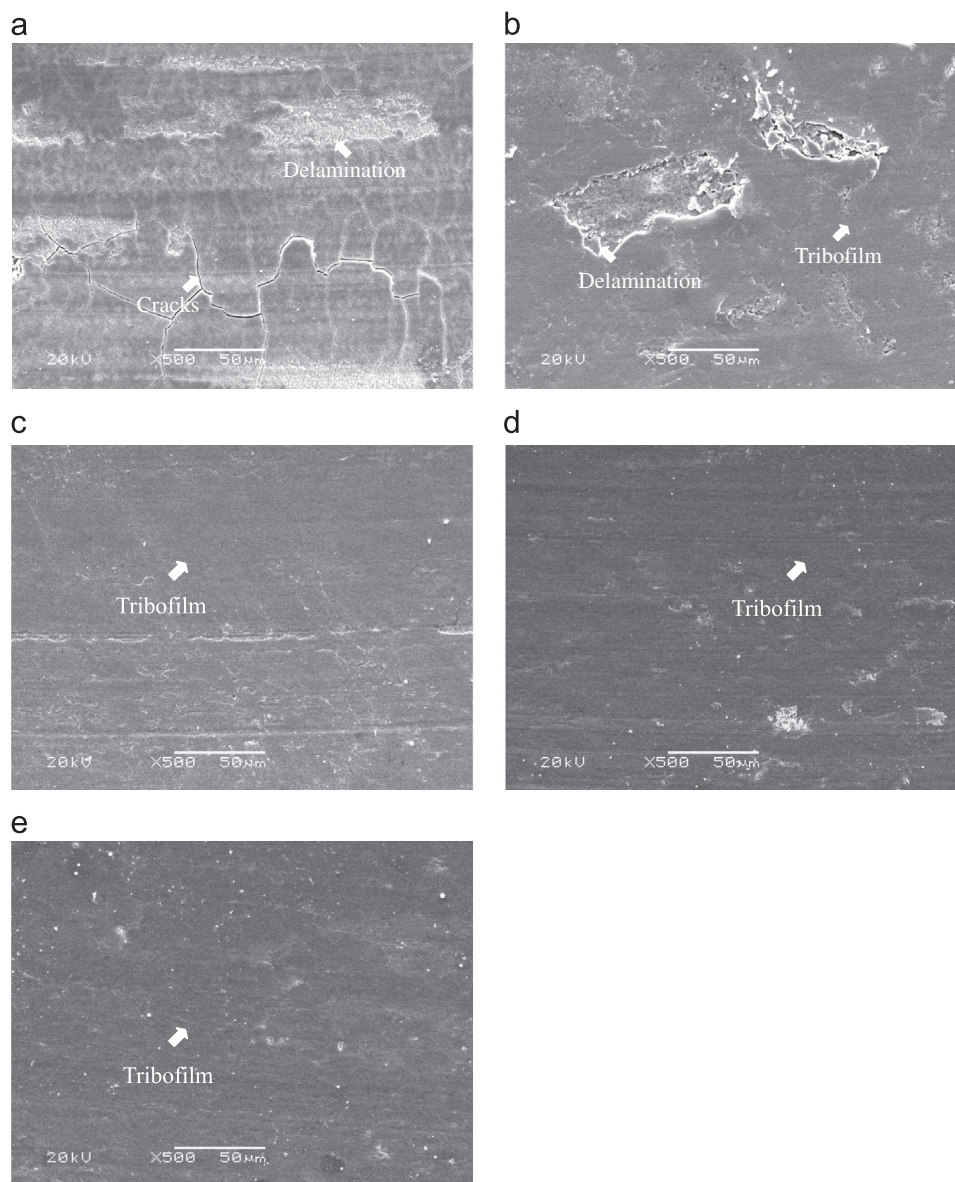


Fig. 6. SEM morphologies of worn surfaces of NC40A–30SrSO<sub>4</sub> composite after wear tests at different temperatures: (a) room temperature, (b) 200 °C, (c) 400 °C, (d) 600 °C, and (e) 800 °C.

temperature at the asperities might be sufficiently high to greatly soften the composites in the tribo-contact region, and the asperities were severely deformed, which resulted in higher wear rate.

In addition, NC40A–SrSO<sub>4</sub> composites with different amounts of SrSO<sub>4</sub> exhibited different synergistic lubricating function over a wide temperature range from room temperature to 800 °C due to the formation of different phases in SrO–Al<sub>2</sub>O<sub>3</sub> system with increasing amount of SrSO<sub>4</sub>. For NC40A–10SrSO<sub>4</sub> composite, SrAl<sub>4</sub>O<sub>7</sub> and NiCr<sub>2</sub>O<sub>4</sub> played an important role in the formation of synergistic lubricating films on the worn surface, which were apparently beneficial to reducing friction coefficient and wear rate of the composite above 200 °C. However, the tribological properties of NC40A–20SrSO<sub>4</sub> and NC40A–30SrSO<sub>4</sub> composites were very poor compared to NC40A–10SrSO<sub>4</sub> composite due to the formation of Sr<sub>4</sub>Al<sub>2</sub>O<sub>7</sub>, SrAl<sub>2</sub>O<sub>4</sub> and NiCr<sub>2</sub>O<sub>4</sub> during sintering process, except the synergistic lubricating effect of Sr<sub>4</sub>Al<sub>2</sub>O<sub>7</sub>,

SrAl<sub>2</sub>O<sub>4</sub> and NiCr<sub>2</sub>O<sub>4</sub> made NC40A–30SrSO<sub>4</sub> composite possess low friction coefficient and wear rate at 400 °C (Fig. 3). It indicated that strontium aluminates (SrAl<sub>4</sub>O<sub>7</sub>, Sr<sub>4</sub>Al<sub>2</sub>O<sub>7</sub>, SrAl<sub>2</sub>O<sub>4</sub>) and NiCr<sub>2</sub>O<sub>4</sub> provided good tribological properties at elevated temperatures.

## 5. Conclusions

NC40A–SrSO<sub>4</sub> composites were prepared by powder metallurgy method, and the tribological properties of the composites were evaluated as a function of the test temperature in the range from room temperature and 800 °C. Results from these studies revealed that:

- (1) The new phases such as SrAl<sub>4</sub>O<sub>7</sub>, Sr<sub>4</sub>Al<sub>2</sub>O<sub>7</sub>, SrAl<sub>2</sub>O<sub>4</sub> and NiCr<sub>2</sub>O<sub>4</sub> formed in the process of hot pressing provided improved tribological properties at elevated temperatures.

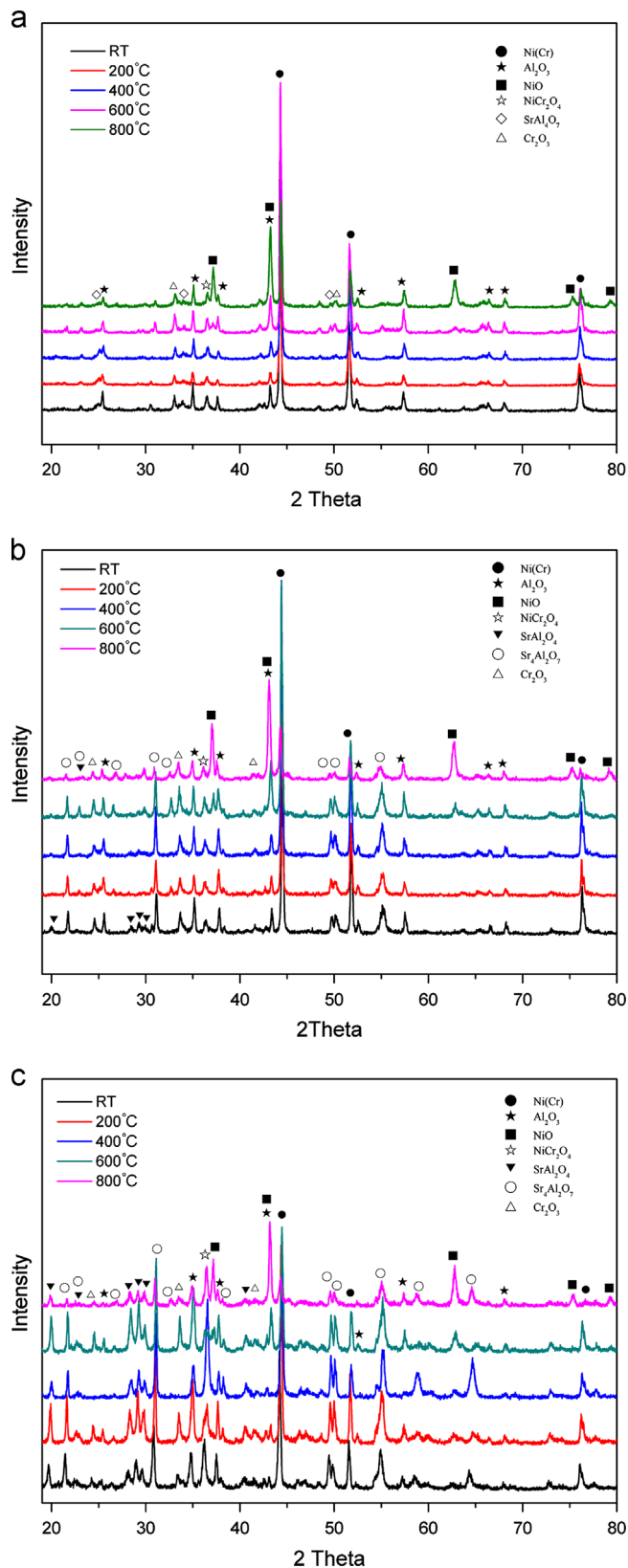


Fig. 7. XRD patterns of worn surfaces of the composites tested at different temperatures: (a) NC40A–10SrSO<sub>4</sub>, (b) NC40A–20SrSO<sub>4</sub>, and (c) NC40A–30SrSO<sub>4</sub>.

(2) For NC40A–SrSO<sub>4</sub> composites, the inclusion of SrSO<sub>4</sub> in NC40A cermet significantly led to a decrease in the friction coefficients and wear rates over a wide temperature

range from 200 °C to 600 °C owing to the formation of synergistic lubricating films of SrAl<sub>4</sub>O<sub>7</sub>, Sr<sub>4</sub>Al<sub>2</sub>O<sub>7</sub>, SrAl<sub>2</sub>O<sub>4</sub> and NiCr<sub>2</sub>O<sub>4</sub> on the worn surface during sliding process.

(3) SrAl<sub>4</sub>O<sub>7</sub> and NiCr<sub>2</sub>O<sub>4</sub> provided good tribological properties in a broad range of the temperature, while Sr<sub>4</sub>Al<sub>2</sub>O<sub>7</sub>, SrAl<sub>2</sub>O<sub>4</sub> and NiCr<sub>2</sub>O<sub>4</sub> endowed NC40A–30SrSO<sub>4</sub> composite with low friction coefficient and wear rate at 400 °C.

## Acknowledgments

The authors acknowledge the financial supports by the National Natural Science Foundation of China (Grant no. 51175490, 51101166) and the “Hundred Talents Program” of Chinese Academy of Sciences (Grant no. KGCX2–YW–804).

## References

- [1] H.E. Sliney, Solid lubricant materials for high-temperatures – a review, *Tribol. Int.* 15 (5) (1982) 303–315.
- [2] A. Erdemir, Solid lubricants and self-lubricating films, in: B. Bhushan (Ed.), *Modern Tribology Handbook*, CRC Press, Boca Raton, FL, 2001, pp. 787–818.
- [3] J.L. Li, D.S. Xiong, Tribological properties of nickel-based self-lubricating composite at elevated temperature and counterface material selection, *Wear* 265 (3–4) (2008) 533–539.
- [4] J.L. Li, D.S. Xiong, M.F. Huo, Friction and wear properties of Ni–Cr–W–Al–Ti–MoS<sub>2</sub> at elevated temperatures and self-consumption phenomena, *Wear* 265 (3–4) (2008) 566–575.
- [5] C.H. Ding, C.H. Liu, Z.M. Yang, Y.P. Wang, Z.B. Sun, L. Yu, Effect of size refinement and distribution of lubricants on friction coefficient of high temperature self-lubricating composites, *Compos. Sci. Technol.* 70 (6) (2010) 1000–1005.
- [6] J.H. Ouyang, S. Sasaki, T. Murakami, K. Umeda, Tribological properties of spark-plasma-sintered ZrO<sub>2</sub>(Y<sub>2</sub>O<sub>3</sub>)–CaF<sub>2</sub>–Ag composites at elevated temperatures, *Wear* 258 (9) (2005) 1444–1454.
- [7] J.H. Ouyang, Y.F. Li, Y.M. Wang, Y. Zhou, T. Murakami, S. Sasaki, Microstructure and tribological properties of ZrO<sub>2</sub>(Y<sub>2</sub>O<sub>3</sub>) matrix composites doped with different solid lubricants from room temperature to 800 °C, *Wear* 267 (9) (2009) 1353–1360.
- [8] Y. Jin, K. Kato, N. Umehara, Effects of sintering aids and solid lubricants on tribological behaviours of CMC/Al<sub>2</sub>O<sub>3</sub> pair at 650 °C, *Tribol. Lett.* 6 (1) (1999) 15–21.
- [9] Y. Jin, K. Kato, N. Umehara, Further investigation on the tribological behavior of Al<sub>2</sub>O<sub>3</sub>–20Ag/20CaF<sub>2</sub> composite at 650 °C, *Tribol. Lett.* 6 (3–4) (1999) 225–232.
- [10] J.H. Ouyang, X.S. Liang, Z.G. Liu, Z.L. Yang, Y.J. Wang, Friction and wear properties of hot-pressed NiCr–BaCr<sub>2</sub>O<sub>4</sub> high temperature self-lubricating composites, *Wear* 301 (1–2) (2013) 820–827.
- [11] A. Erdemir, A crystal-chemical approach to lubrication by solid oxides, *Tribol. Lett.* 8 (2–3) (2000) 97–102.
- [12] C. Donnet, A. Erdemir, Solid lubricant coatings: recent developments and future trends, *Tribol. Lett.* 17 (3) (2004) 389–397.
- [13] S.D. Walck, M.S. Donley, J.S. Zabinski, V.J. Dyhouse, Characterization of pulsed-laser deposited PbO/MoS<sub>2</sub> by transmission electron-microscopy, *J. Mater. Res.* 9 (1) (1994) 236–245.
- [14] S.D. Walck, J.S. Zabinski, N.T. McDevitt, J.E. Bultman, Characterization of air-annealed, pulsed laser deposited ZnO–WS<sub>2</sub> solid film lubricants by transmission electron microscopy, *Thin Solid Films* 305 (1) (1997) 130–143.
- [15] W. Gulbinski, T. Suszko, W. Sienicki, B. Warcholinski, Tribological properties of silver- and copper-doped transition metal oxide coatings, *Wear* 254 (1–2) (2003) 129–135.



- [16] A. Ozturk, K.V. Ezirmik, K. Kazmanli, M. Urgan, O.L. Eryilmaz, A. Erdemir, Comparative tribological behaviors of TiN-, CrN- and MoN-Cu nanocomposite coatings, *Tribol. Int.* 41 (1) (2008) 49–59.
- [17] S.M. Aouadi, Y. Paudel, B. Luster, S. Stadler, P. Kohli, C. Muratore, C. Hager, A.A. Voevodin, Adaptive Mo<sub>2</sub>N/MoS<sub>2</sub>/Ag tribological nanocomposite coatings for aerospace applications, *Tribol. Lett.* 29 (2) (2008) 95–103.
- [18] S.M. Aouadi, Y. Paudel, W.J. Simonson, Q. Ge, P. Kohli, C. Muratore, A.A. Voevodin, Tribological investigation of adaptive Mo<sub>2</sub>N/MoS<sub>2</sub>/Ag coatings with high sulfur content, *Surf. Coat. Technol.* 203 (10–11) (2009) 1304–1309.
- [19] S.M. Aouadi, D.P. Singh, D.S. Stone, K. Polychronopoulou, F. Nahif, C. Rebholz, C. Muratore, A.A. Voevodin, Adaptive VN/Ag nanocomposite coatings with lubricious behavior from 25 to 1000 °C, *Acta Mater.* 58 (16) (2010) 5326–5331.
- [20] P. John, S. Prasad, A. Voevodin, J. Zabinski, Calcium sulfate as a high temperature solid lubricant, *Wear* 219 (2) (1998) 155–161.
- [21] Z. Liu, Elevated temperature diffusion self-lubricating mechanisms of a novel cermet sinter with orderly micro-pores, *Wear* 262 (5) (2007) 600–606.
- [22] Y. Wang, Z. Liu, Tribological properties of high temperature self-lubrication metal ceramics with an interpenetrating network, *Wear* 265 (11) (2008) 1720–1726.
- [23] F. Liu, J.H. Jia, Tribological properties and wear mechanisms of NiCr-Al<sub>2</sub>O<sub>3</sub>-SrSO<sub>4</sub>-Ag self-lubricating composites at elevated temperatures, *Tribol. Lett.* 49 (1) (2013) 281–290.
- [24] M. Capron, A. Douy, Strontium dialuminate SrAl<sub>4</sub>O<sub>7</sub>: synthesis and stability, *J. Am. Ceram. Soc.* 85 (12) (2002) 3036–3040.
- [25] S.J. Kim, H.I. Won, N. Hayk, C.W. Won, D.Y. Jeon, A.G. Kirakosyan, Preparation and characterization of Sr<sub>4</sub>Al<sub>2</sub>O<sub>7</sub>:Eu<sup>3+</sup>, Eu<sup>2+</sup> phosphors, *Mater. Sci. Eng. B-Adv.* 176 (18) (2011) 1521–1525.
- [26] X.Y. Ye, W.D. Zhuang, J.F. Wang, W.X. Yuan, Z.Y. Qiao, Thermodynamic description of SrO-Al<sub>2</sub>O<sub>3</sub> system and comparison with similar systems, *J. Phase Equilib. Diff.* 28 (4) (2007) 362–368.
- [27] P. Escribano, M. Marchal, M.L. Sanjuan, P. Alonso-Gutierrez, B. Julian, E. Cordoncillo, Low-temperature synthesis of SrAl<sub>2</sub>O<sub>4</sub> by a modified sol-gel route: XRD and Raman characterization, *J. Solid State Chem.* 178 (6) (2005) 1978–1987.